Molecular Microbiology (2012) 83(6), 1136–1152 ■
doi:10.1111/j.1365-2958.2012.07996.x
First published online 14 February 2012

The role of flotillin FloA and stomatin StoA in the maintenance of apical sterol-rich membrane domains and polarity in the filamentous fungus *Aspergillus nidulans*

Norio Takeshita,[1]* George Diallinas[2] and Reinhard Fischer[1]
[1]*Karlsruhe Institute of Technology (KIT), Institute for Applied Biosciences, Dept. of Microbiology, Hertzstrasse 16, D-76187 Karlsruhe, Germany.*
[2]*Faculty of Biology, Athens University, Panepistimioupolis 15781, Athens, Greece.*

Summary

Apical sterol-rich plasma membrane domains (SRDs), which can be viewed using the sterol-binding fluorescent dye filipin, are gaining attention for their important roles in polarized growth of filamentous fungi. The microdomain scaffolding protein flotillin/reggie and related stomatin were thought to be good candidates involved in the formation of SRDs. Here, we show that the flotillin/reggie orthologue FloA tagged with GFP localized as stable dots along the plasma membrane except hyphal tips. Deletion of *floA* reduced the growth rate, often resulted in irregularly shaped hyphae and impaired SRDs. In contrast, the stomatin orthologue StoA, tagged with GFP, localized at the cortex of young branch tips and at the subapical cortex in long hyphal tips, and was transported bi-directionally along microtubules on endosomes. Deletion of *stoA* resulted in irregular hyphal morphology and increased branching especially in young hyphae, but did not obviously affect SRDs. Double deletion of *floA* and *stoA* enhanced the defects of growth and hyphal morphology. Our data suggest that the plasma membrane of hyphal tips and in subapical regions are distinct and that FloA is involved in membrane compartmentalization and probably indirectly in SRD maintenance.

Introduction

Filamentous fungi grow by continuous tip elongation and branching, forming hyphae and mycelium. Hyphal tip growth requires continuous transport of secretory vesicles in order to supply the proteins and lipids necessary for the extension of the cell wall and membrane (Harold, 1999). The highly polarized growth of filamentous fungi depends on the microtubule and actin cytoskeletons, along with their associated motor proteins (Fischer *et al*., 2008; Steinberg, 2011). Apical membrane-associated landmark proteins, so-called 'cell end markers', link these two cytoskeletons in *Aspergillus nidulans* (Takeshita *et al*., 2008; Higashitsuji *et al*., 2009; Takeshita and Fischer, 2011). Furthermore, there is some indication that apical sterol-rich plasma membrane domains play an important role in polarized growth and localization of cell end markers (Takeshita *et al*., 2008).

Eukaryotic membranes are differentiated into different functional areas (Rothberg *et al*., 1990; Rajendra and Simons, 2005; Lingwood and Simons, 2010). Sterols and sphingolipids can cluster into domains within mixtures of glycerophospholipids. These domains, termed 'lipid rafts', contribute to specific protein localization at specific sites, such as GPI-anchored and lipid-associated proteins, and play important roles in cell signalling and cell polarity (Simons and Toomre, 2000; Schuck and Simons, 2004; Stuermer, 2010). One type of domain, characterized by a high sterol content, is found in fungi (Alvarez *et al*., 2007). Sterol-rich membrane domains (SRDs) were visualized using the sterol-binding fluorescent dye filipin. This dye stained the tips of mating projections in *Saccharomyces cerevisiae* (Bagnat and Simons, 2002) and *Cryptococcus neoformans* (Nichols *et al*., 2004), as well as cell ends in *Schizosaccharomyces pombe* (Wachtler *et al*., 2003), and hyphal tips in *Candida albicans* (Martin and Konopka, 2004) and *A. nidulans* (Pearson *et al*., 2004).

The most abundant sterol found in fungi is ergosterol, which forms rafts better than cholesterol (Xu *et al*., 2001). In both yeast and mammalian cells, sterols are mainly synthesized *de novo* in the ER membrane and are transported to the plasma membrane by vesicular and non-vesicular transport (Urbani and Simoni, 1990; Baumann *et al*., 2005). Recently, it has been shown that SRDs contribute to polar growth in *C. albicans* (Martin and Konopka, 2004) and *A. nidulans* (Pearson *et al*., 2004; Li *et al*., 2006; Takeshita *et al*., 2008); however, the role and

Accepted 25 January, 2012. *For correspondence. E-mail norio.takeshita@kit.edu; Tel. (+49) 721 608 44635; Fax (+49) 721 608 44509.

formation mechanism of SRDs remain elusive (Alvarez *et al*., 2007). The size of SRDs in fungi is around a few μm, depending on the organism, which is much bigger in size than lipid rafts, which range between 10 and 200 nm (Pike, 2009). The SRDs are specific to fungi and their presence has not been reported in mammalian cells, suggesting not only fungal specific roles in membrane organization, but also potential targets for antifungal drugs (Mania *et al*., 2010).

Clustering of lipid rafts is thought to be involved in the formation of SRDs. There are numerous studies on raft formation in different organisms, and some components are known. Flotillin/reggie proteins, for instance, are known to form microdomains at the plasma membrane (Stuermer, 2010). Reggie was discovered in neuron proteins upregulated during axon regeneration and was necessary for axon growth (Munderloh *et al*., 2009), whereas flotillin was independently identified as a marker for lipid rafts (Bickel *et al*., 1997). The flotillin/reggie orthologues are highly conserved in metazoa, and flotillin/reggie-like proteins are present also in bacteria (Hinderhofer *et al*., 2009) and plants (Borner *et al*., 2005). The N-terminal half of the protein comprises a hydrophobic domain and attaches to the cytoplasmic face of the membrane, while the C-terminal portion is required for homo- and hetero-oligomer formation (Browman *et al*., 2007) (Fig. 1A). During axon growth, flotillin/reggie is suggested to induce membrane microdomain formation at the tip cortex (Morrow *et al*., 2002; Langhorst *et al*., 2008; Stuermer, 2011). These microdomains in turn result in an accumulation of specific proteins at the tip cortex (Langhorst *et al*., 2008; Stuermer, 2010; 2011). Furthermore, flotillin/reggie appear to be involved in cell division, Alzheimer and Parkinson disease, and other phenomena (Santamaria *et al*., 2005; Babuke and Tikkanen, 2007). The N-terminal half of the membrane-associated domain of flotillin/reggie is conserved in stomatin, prohibitin and HflK; these are called SPFH domains (Browman *et al*., 2007). Proteins containing SPFH domains are found in lipid rafts in diverse cellular membranes, suggesting that they function within different and specific organelle membranes (Browman *et al*., 2007).

Stomatin family proteins are widely distributed in eukaryotes, bacteria and archaea (Green and Young, 2008). Stomatin is palmitoylated and is integrated in the membrane in its oligomeric form (Snyers *et al*., 1998). In human cells, it is associated with rafts (Snyers *et al*., 1999). It was initially identified in the red cell plasma membrane, but experimental studies show that its subcellular location extends intracellular membranes such as endosomes (Snyers *et al*., 1999; Mairhofer *et al*., 2009). The stomatin family proteins are thought to perform specific scaffolding functions in membranes, especially the plasma membrane and endosomes in human cells (Morrow and Parton, 2005; Mairhofer *et al*., 2009).

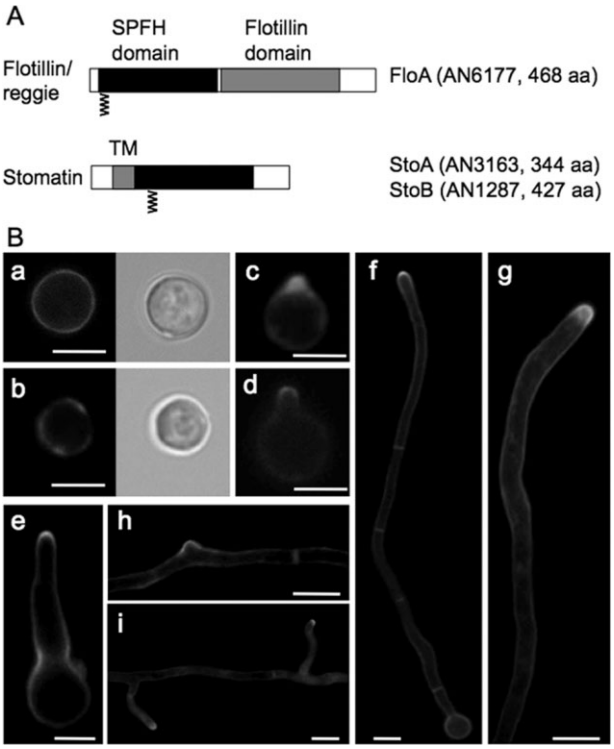

Fig. 1. Structure of flotillin and stomatin.
A. The SPFH domain is conserved in the flotillin orthologue FloA, and stomatin orthologues StoA and StoB. The stomatin homologous proteins possess a transmembrane domain at the N-terminal side of the SPFH domain. There are putative palmitoylation sites in FloA (Cys4) and StoA (Cys79).
B. SRDs at polarity sites. The spores of wild-type strain (TN02A3) were grown in minimal medium with glucose overnight. Germlings and hyphae were stained using filipin at 1 μg ml^{-1} for 5 min. SRDs were observed at tips of germtubes (c–e), branches (h and i), hyphae (f and g) and at septa (f and h). Scale bars = 5 μm.

In order to analyse the functional roles of SRDs in the filamentous fungus *A. nidulans*, we investigated the mechanism of SRD formation and/or maintenance. The microdomain scaffolding protein flotillin/reggie and the related stomatin were chosen as candidates involved in SRD formation. Here, we analysed the function of two stomatin orthologues, StoA and StoB, and the flotillin/reggie orthologue FloA.

Results

SRDs at polarity sites and at septa

In order to investigate SRDs in *A. nidulans*, germlings and hyphae were stained using 1 μg ml^{-1} filipin for 5 min. While cell incubation in high filipin concentrations or longer durations has been shown to alter sterol-containing membrane regions and disrupt their functions (Wachtler *et al*., 2003), a concentration of 1 μg ml^{-1} filipin with overnight exposure does not affect germination and hyphal morphology in *A. nidulans* (Takeshita *et al*., 2008). We compared filipin-

staining images at different growth stages. SRDs were observed at the tips of germtubes (Fig. 1Bc–e), branch sites (Fig. 1Bh), tips of hyphae (Fig. 1Bf and g), and also at septa (Fig. 1Bf and h). Prior to germination, the signal appeared uniformly at the cortex in some spores (Fig. 1Ba), but there were also spores showing patchy signals around the cortex (Fig. 1Bb). At the small tips during germination and branch formation, the signal appeared widely at the tip membrane (Fig. 1Bc and h). Depending on the growth of the germtube and the branch, the signal tended to concentrate at the apex (Fig. 1Bd and i). The signal at the tips of young germtubes was weaker and narrower at the apex than those of mature, long hyphae (Fig. 1Bd–g), suggesting that SRDs develop as hyphae elongate, alternatively, that the relative accessibility of filipin is different between these sites.

SPFH proteins in A. nidulans

The first insights into the mechanism responsible for SRD formation and maintenance in filamentous fungi were obtained by analysing the *A. nidulans* genome for orthologues of the microdomain-scaffolding proteins flotillin/reggie and stomatin. To this end, the *A. nidulans* database (http://www.aspgd.org) was searched for human flotillin-1. The open reading frame with the highest similarity score was AN6177. The corresponding predicted protein comprised both a SPFH domain and a flotillin domain (Fig. 1A). The identity between *A. nidulans* AN6177 and human flotillin-1 was only 25% with an *e*-value of 5e-09. The putative flotillin orthologue was named FloA (Fig. 1A). The alignment and a phylogenetic relationship of flotillin orthologues are shown in Supplemental Data 1 (Fig. S1). We found highly similar proteins in ascomycetous filamentous fungi, with 74–83% identity in other Aspergilli and 42% identity in *Neurospora crassa.* The protein was not identified in *S. cerevisiae*, *S. pombe*, *Ashbya gossypii*, *C. albicans*, Basidiomycota or Zygomycota. In addition to FloA, four other SPFH-containing proteins with similarity to stomatin and prohibitin were identified. Two proteins with similarity to human stomatin were AN3163, with 32% identity and an *e*-value of 9e-31, and AN1287, with 30% and an *e*-value of e-21. We named them StoA and StoB respectively (Fig. 1A). Two putative orthologues were identified for prohibitin (AN0686 and AN6073). Since prohibitins are known to localize at the mitochondrial inner membrane and function as mitochondrial chaperones (Mishra *et al.*, 2006), only FloA, StoA and StoB were selected for further investigations in this study. FloA and StoA contained putative palmitoylation motifs (in FloA at Cys4; in StoA at Cys79), similar to human flotillin/reggie and stomatin (Fig. 1A) (identified by CSS-Palm 3.0 algorithm). Palmitoylation of flotillin/reggie was shown to be important for their localization to lipid raft domains (Morrow *et al.*, 2002).

Flotillin FloA localization

To investigate the localization of FloA, GFP was fused to the C-terminus of FloA, and FloA–GFP expressed under the control of the *alcA* promoter which is regulatable through the carbon source. We constructed strains expressing FloA–GFP instead of native FloA. The fusion protein proved to be biologically functional, because effects such as growth delay or abnormal hyphal morphology – observed in *floA*-deletion strains (see below) – were not obvious in the strain expressing FloA–GFP. Under derepressed conditions with glycerol as carbon source, FloA–GFP localized to the cortex along the hyphae, except hyphal tips (Fig. 2A and B). The signal was not uniform along the cortex, but appeared as aligned dots. Mammalian flotillin/reggie localize to the membrane because they are palmitoylated proteins. The localization pattern of FloA–GFP in *A. nidulans* strongly suggests that FloA localizes to the plasma membrane. The signal intensity of GFP was stronger close to the spores, and gradually became weaker towards hyphal tips. Interestingly, the protein appeared to be completely absent from the apical membranes where SRDs were observed (Fig. 2A and D). FloA–GFP did not localize to branch tips (Fig. 2C arrows) and septa (Fig. 2C arrowheads). The dots of FloA–GFP appeared to be immobile (Fig. 2D kymograph, Movies S1 and S2).

To investigate any effect of the expression under the *alcA* promoter on the localization of FloA–GFP, the *alcA* promoter was replaced by the 2 kb *floA* putative promoter region. Only faint GFP signal dots were observed along the hyphal cortex except hyphal tips; however, in contrast to FloA–GFP expressed under the *alcA* promoter, a clear signal accumulation close to the spores was not observed. Furthermore, FloA–GFP expressed under the constitutive *gdpA* promoter showed a subcellular localization identical to that obtained with the *alcA* promoter (data not shown).

In earlier experiments, GFP was fused to FloA lacking 46 amino acids at the C-terminus (FloAΔC) because the gene had been misannotated in the *A. nidulans* database, where one exon was missing. The correct gene structure has meanwhile been confirmed by cDNA sequencing in RNAseq experiments. The truncated FloAΔC–GFP was expressed under the native promoter and surprisingly localized to the hyphal tip cortex (Fig. 2E and F). This tip localization was opposite to the localization of full length FloA–GFP. This discrepancy could be due to artefacts because of the GFP molecule attached to the C-terminus. On the other hand, it could be that the 46 amino acids are important for correct localization or even could be involved in a regulatory mechanism. In order to confirm the localization of the full-length protein, we studied N-terminally tagged FloA.

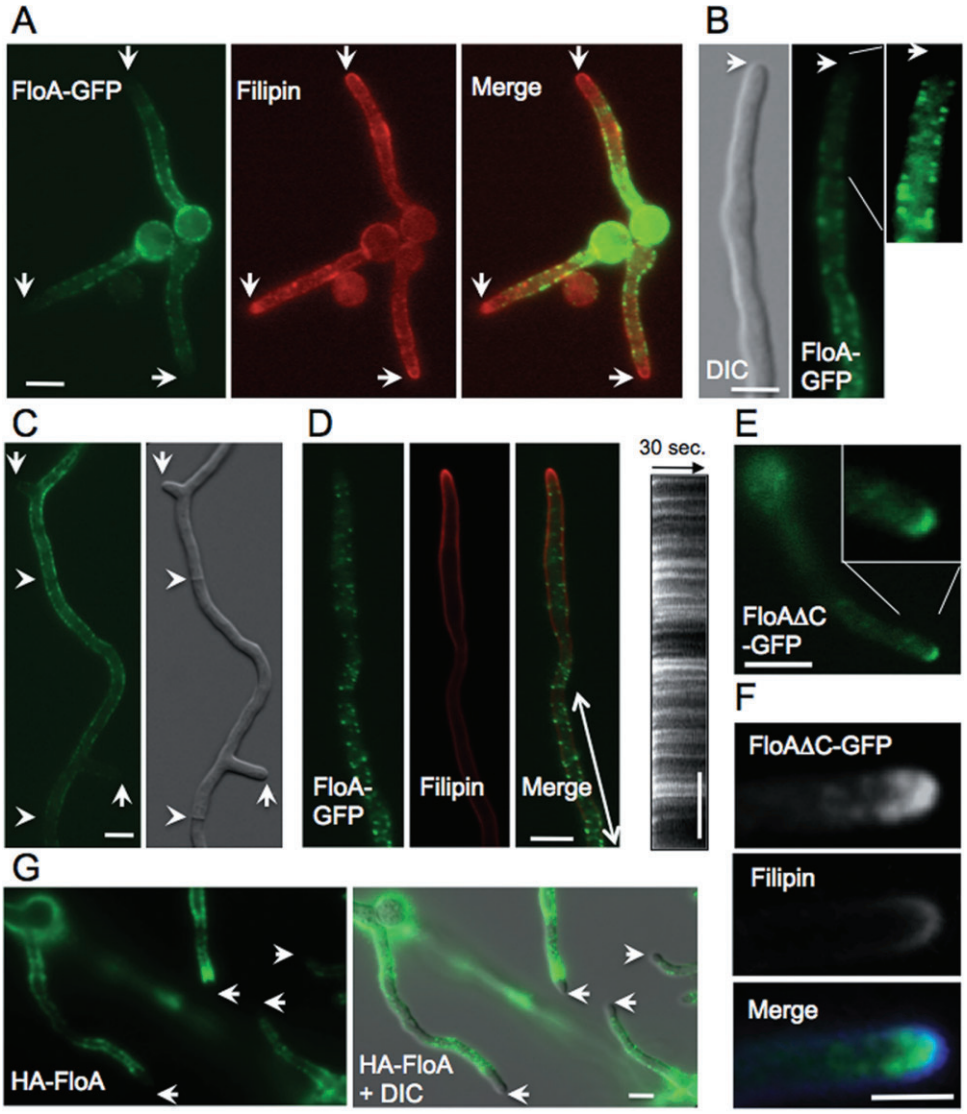

Fig. 2. Localization of FloA. (A–E) The strain expressing functional FloA-tagged GFP at the C-terminus under the control of the *alcA* promoter, was grown in minimal medium with glycerol overnight. FloA–GFP localized to plasma membrane as dots through hyphae except hyphal tips (A and B, arrows indicate hyphal tips). (A and D) Hyphae were stained using filipin at 1 μg ml^{-1} for 5 min. The FloA–GFP did not localize to SRDs (arrows indicate hyphal tips). (C) FloA–GFP did not localize to branch tips (arrows) or septa (arrowheads). (D) The dots of FloA–GFP appeared to be immobile. The Kymograph was made with ImageJ on a segmented line (not shown) along the hyphal cortex restricted by the arrow line. Vertical bars = μm, horizontal arrow = 30 s. (E and F) The strain expressing FloAΔC–GFP under the control of the native promoter was grown in minimal medium with glucose overnight. The FloAΔC–GFP accumulated at hyphal tips and the apical cortex (E). (F) Comparison of FloA–GFP and SRDs stained by filipin. Hyphae were stained using filipin at 1 μg ml^{-1} for 5 min. (G) Indirect immunofluorescence stain of HA–FloA expressed under the control of the native promoter. HA–FloA localized to the plasma membrane along hyphae except at hyphal tips (arrows indicate hyphal tips). Scale bars = 5 μm.

We constructed N-terminally GFP-tagged FloA and expressed it under the control of the *alcA* promoter. Under repressed conditions with glucose as carbon source, the strain showed a growth delay and similar abnormal hyphal morphology as *floA*-deletion strains (see below). Under derepressed conditions with glycerol as carbon source, the hyphal morphology phenotype was not rescued although the growth delay was partially suppressed. GFP–FloA did not localize to the plasma membrane but appeared as oscillating small dots in the cytoplasm (data not shown). These data indicate that the N-terminal GFP fusion of FloA is not functional. This may indicate that the putative N-terminal palmitoylation at Cys4 is important for its localization to the membrane and /or for function.

Next, FloA was fused to three repeats of HA at the N-terminus and HA–FloA expressed instead of native FloA under the 2 kb *floA* putative promoter region. The

fact that the strain did not display any growth delay or hyphal morphology phenotype proved that HA–FloA is biologically functional. The localization of HA–FloA was investigated by indirect immunofluorescence. FITC signals were detected as dots along the hyphal cortex except hyphal tips (Fig. 2G) and a clear signal accumulation close to spores was not observed. In agreement with the GFP-localization studies described above, we conclude that the functional FloA protein localizes along the hyphal cortex but is excluded from the hyphal tip.

floA *deletion*

To analyse the biological function of *floA*, we constructed a *floA*-deletion strain (see *Experimental procedures*). The colony diameter of the *floA*-deletion strain was smaller than that of wild type (60–70%) (Fig. 3A and B). Hyphae in the *floA*-deletion strain exhibited abnormal morphology with typically irregular hyphal widths (Fig. 3C–H). The hyphal widths in the *floA*-deletion and wild-type strain were measured in 10 μm increments from the tip (Fig. 3I). The means of hyphal widths at nine points is displayed in Fig. 3J. The standard deviation in the wild-type strain was mostly lower than 0.3 μm (90% of hyphe, $n = 20$). In contrast, the standard deviation in the *floA*-deletion strain was 0.3–0.7 μm ($n = 20$). These data reflect the irregular hyphal morphology. In addition, sometimes protrusions (Fig. 3K arrowhead) and ruffled hyphae (Fig. 3K arrows) were observed along hyphae of the *floA*-deletion strain. There was no obvious difference in the frequency of branch formation and septation.

SRD integrity and localization of polarity-associated proteins depend on floA

The orthologue of flotillin was expected to be involved in the formation of membrane domains, although FloA did not localize to SRDs but plasma membrane except SRDs. Nevertheless, the hyphal morphology of the *floA*-deletion strain suggest the impair in the proper hyphal tip growth. Therefore, the *floA*-deletion strain was stained using filipin to investigate the effect of *floA* deletion on SRD formation (Fig. 4A). Clear signals of SRDs were observed in 60% of hyphae (Fig. 4Aa). In 40% of the hyphae, SRDs were observed at tips, but the filipin signals diffused to subapical regions too (Fig. 4Ab), or SRDs were not clearly detected at tips and the signals diffused and accumulated in subapical regions (Fig. 4Ac and B). These data suggest that FloA is involved in the maintenance of SRDs; however, the contribution of FloA is indirect because FloA localized to plasma membrane except SRDs.

Previous findings indicated that SRDs are necessary for the localization of the cell end markers TeaA and TeaR (Takeshita *et al*., 2008). In the wild type, both mRFP1-tagged TeaA and GFP-tagged TeaR accumulated at the hyphal tip apex (Fig. 5A and B). TeaR is a prenylated protein and attaches to the plasma membrane at the cortex tip through the prenyl residue. In general, prenylated proteins are thought to be excluded from rafts (Melkonian *et al*., 1999). We assume thus that TeaR is attached to non-raft membrane regions. GFP–TeaR sometimes located at some spots aligned along the apical membrane (Fig. 5B) (Takeshita *et al*., 2008). In order to further verify whether FloA is involved in the formation of SRDs, localization of TeaA and TeaR was analysed in the *floA*-deletion strain (Fig. 5C and D), where TeaR dots spread to subapical regions (Fig. 5C) and to the cortex of subapical and/or backward protrusions and ripples of hyphae (Fig. 5C). Since the localization of TeaA and TeaR is interdependent (Takeshita *et al*., 2008), likewise, TeaA also mislocalized to subapical regions of hyphae. These data are consistent with the idea that FloA is involved in the formation of SRDs. Moreover, the mislocalization of cell end markers to subapical region correlated with the absence of SRDs. At the tips of hyphae where no clear SRDs were observed, both TeaA and TeaR often showed dispersed signals at the subapical cortex of more than 80% of the tips ($n = 100$) (Fig. 5D and E). In contrast, at the tips of hyphae in the presence of SRDs, cell end markers mislocalized in 20% of the tips ($n = 100$) (Fig. 5E). This apparent correlation of SRD integrity and cell end marker localization suggests the importance of SRDs. The observed mislocalization of cell end markers in the presence of SRDs suggests the limit of filipin staining that may only detect severe defects of SRDs.

StoA localization

Localization of the putative stomatin orthologue StoA was investigated by fusing GFP to the C-terminus of StoA using the fusion PCR strategy (Szewczyk *et al*., 2006). StoA–GFP was expressed under the native promoter and also showed biological activity, since hyphae looked like wild-type hyphae and did not show any abnormality as the *stoA* loss-of-function strain did (see below). StoA–GFP concentrated at the tip cortex of young branch tips (Fig. 6Aa), but changed the localization to the subapical cortex depending on the length of the branches (Fig. 6Ab). After hyphae reached a certain length, StoA–GFP transferred to the subapical cortex, but not the apex (Fig. 6Ac). In addition, StoA–GFP localized to cytoplasmic punctate structures that appear as two different classes according to their size and movement. The smaller spots often moved bidirectionally for long distances (Fig. 6B, Movies S3 and S4). In contrast, the larger and less abundant spots showed only short-range movement (Fig. 6B right arrowheads). The ratio of the two classes of

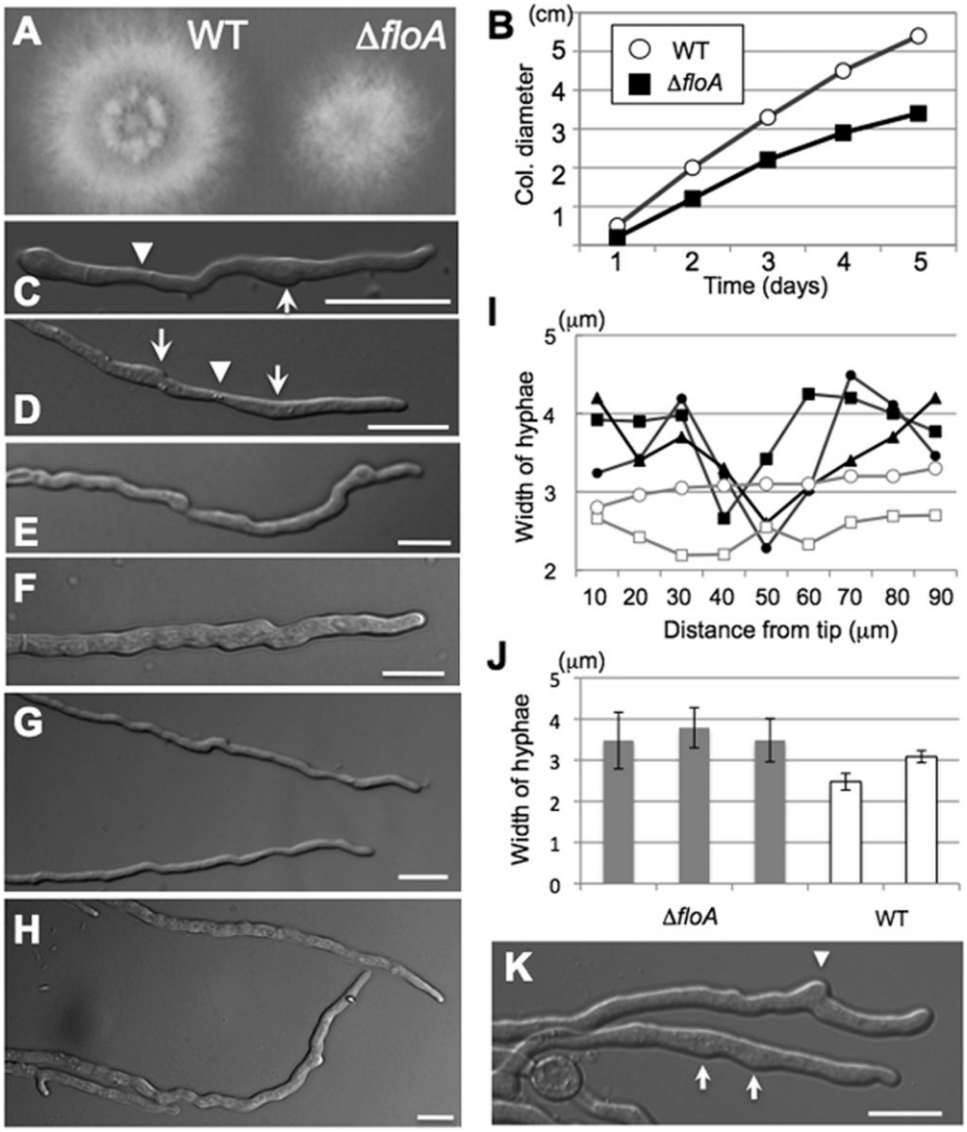

Fig. 3. Deletion of *floA*.
A. Colonies of wild type (left) and the *floA*-deletion (right) strain. The strains were grown in minimal medium with glucose agar plates for 3 days at 37°C.
B. Colony diameter of wild type (white circle) and the *floA*-deletion (black square) strain were measured every day for 5 days at 37°C.
C–H. The *floA*-deletion strain was grown in minimal medium with glucose overnight at 28°C. (C–F) Along hyphae, some parts were wider (arrows), while other parts were narrower (arrowhead). (G and H) Hyphal width changes appeared repeatedly.
I. The width of hyphae at several points from the tip in wild type (open symbols, two hyphae) and the *floA*-deletion (closed symbols, three hyphae) strain. The width of hyphae was not constant in the *floA*-deletion strain in comparison to wild type.
J. The means of hyphal widths at several points from the tip ± standard deviation ($n = 9$).
K. Protrusions (arrowhead) and ripples occurred occasionally along hyphae (arrows).
Scale bars = 10 μm.

StoA–GFP varied in different hyphae. In a small number of hyphae, StoA–GFP did not localize at the subapical cortex, but at endosomal structures (Fig. 6Ad). In old compartments of hyphae, the GFP signal located in vacuole-like structures (Fig. 6Ae).

The velocity of the StoA–GFP small spots was measured from the data of a kymograph (Fig. 6B), 1.28 ± 0.28 μm s^{-1} for anterograde ($n = 20$) and 1.22 ± 0.28 μm s^{-1} for retrograde transport ($n = 20$). Microtubules were visualized by mcherry tagged α-tubulin (TubA) and compared to the StoA–GFP movement. The spots of StoA–GFP appeared to move bidirectionally along microtubules (Fig. 6C) and the movement of StoA resembled the movement of endosomes (Abenza *et al.*, 2009; 2010). Therefore, the localization of StoA was compared to GFP-tagged RabA, which is a marker for endo-

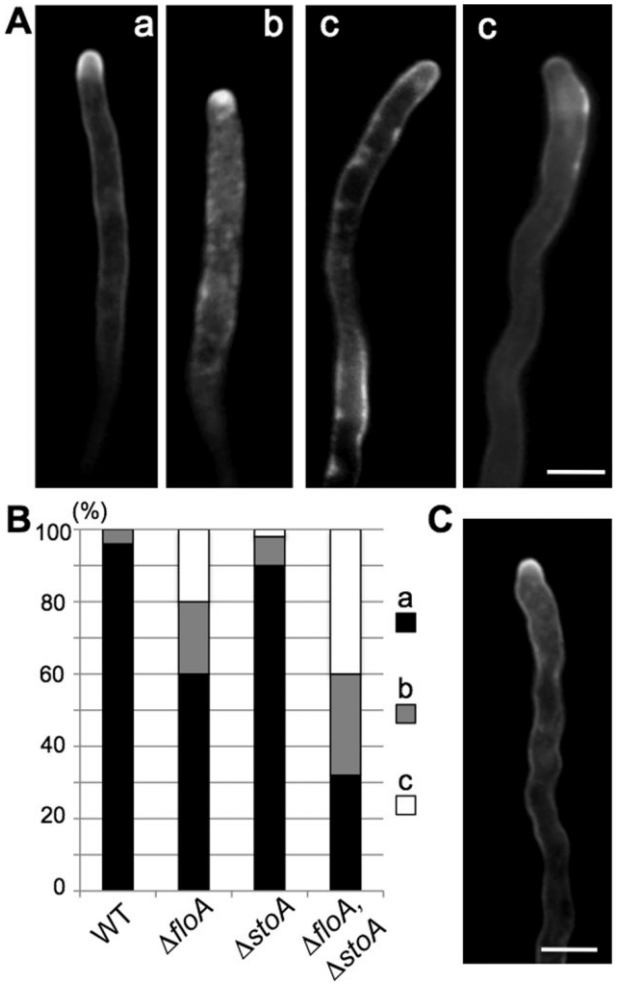

Fig. 4. SRDs in a *floA*-deletion strain. (A and C) The *floA*-deletion strain (A) and the *stoA*-deletion strain (C) were grown in minimal medium with glucose overnight. Hyphae were stained using filipin 1 μg ml^{-1} for 5 min. (A) SRDs were observed at some tips (a), but at other tips filipin signals also diffused to subapical regions (b). At other tips of hyphae, SRDs were not clearly detected and the signals diffused to subapical regions (c). Scale bars = 5 μm. (B) Quantitative analysis of the filipin staining classified into three groups (a–c): wild type ($n = 50$), *floA*-deletion ($n = 100$), *stoA*-deletion strain ($n = 50$) and *floA*, *stoA* double-deletion strain ($n = 100$). (C) SRDs were observed at the majority of hyphal tips, even if the hyphae exhibited abnormal morphology. Scale bars = 5 μm.

somes (Abenza *et al*., 2009; 2010). Here, we used StoA tagged by mRFP1 at the N-terminus, expressed under *alcA* promoter control. The N-terminally tagged version appeared to display the same movement as the C-terminally tagged protein. Indeed, StoA and RabA colocalized at the smaller spots (Fig. 6D left arrowheads). Colocalization was also visualized in corresponding kymographs (Fig. 6D right). The bidirectional transport of endosomes along microtubules depends on kinesin-3 (UncA in *A. nidulans*) and dynein in filamentous fungi (Abenza *et al*., 2009; 2010; Zekert and Fischer, 2009; Schuster *et al*., 2011). Therefore, the dynamics of StoA–GFP was analysed using a *nudA* (dynein heavy chain)-deletion strain and an *uncA*-deletion strain. GFP–RabA is known to accumulate at tips of hyphae in the *nudA* mutant (Abenza *et al*., 2009). StoA–GFP as well as RabA showed the accumulation at almost all tips in the *nudA*-deletion strain (Fig. 6E). In the *uncA*-deletion strain, StoA–GFP localized at the subapical cortex and at cytoplasmic dots; however, while the dots just oscillated, structures moving bidirectionally for long distances were not observed (Fig. 6F, Movie S5). These data indicate that StoA is transported on endosomes.

stoA *deletion and SRD formation*

In order to investigate the function of *stoA*, we constructed a *stoA*-deletion strain (see *Experimental procedures*). The colony diameter of the *stoA*-deletion strain was slightlysmaller than that of the wild type (Fig. 7A). Hyphae of the *stoA*-deletion strain were significantly thicker than wild-type hyphae (Fig. 7B) and grew irregularly (Fig. 7C) especially in young hyphae grown for 1 day. The lateral branching frequency appeared to be higher in hyphae of *stoA*-deletion strains (Fig. 7D and E). When branched hyphae were observed in wild-type hyphae, one branch always appeared from one compartment between neighbour septa ($n = 50$). In contrast, there were sometimes two branches and even three or four, including short branch tips, in hyphae of the *stoA*-deletion strain (Fig. 7F). Compartments in *stoA*-deletion strains looked also smaller than those of wild type (Fig. 7E arrows). To quantify the distance between neighbouring septa, the distances between the first septum and the second septum in germtubes from spores were measured. Germlings were chosen in order to avoid different growth speeds in mature hyphae. Whereas wild-type compartments showed a normal size distribution with a peak at 15–20 μm and only 4% of the compartments were shorter than 10 μm, compartments of the *stoA*-deletion strain showed the peak at 10–15 μm, and 26% of the compartments were shorter than 10 μm (Fig. 7G). Although the smaller compartments in the absence of StoA could be a reason for increased branch formation, StoA localization at the tip cortex of young branches in combination with the branching phenotype suggests that StoA is more directly involved in branch formation. These abnormal phenotypes became weaker with time and hyphae continued to grow similar to wild type.

Subsequently, we investigated the effect of *stoA* deletion on SRD formation by filipin staining (Fig. 4C). Although hyphae appeared abnormal in the *stoA*-deletion strain, SRDs were observed at more than 90% of the tips of hyphae (Fig. 4B). In contrast to FloA, StoA appeared to be unnecessary for SRD formation and/or maintenance.

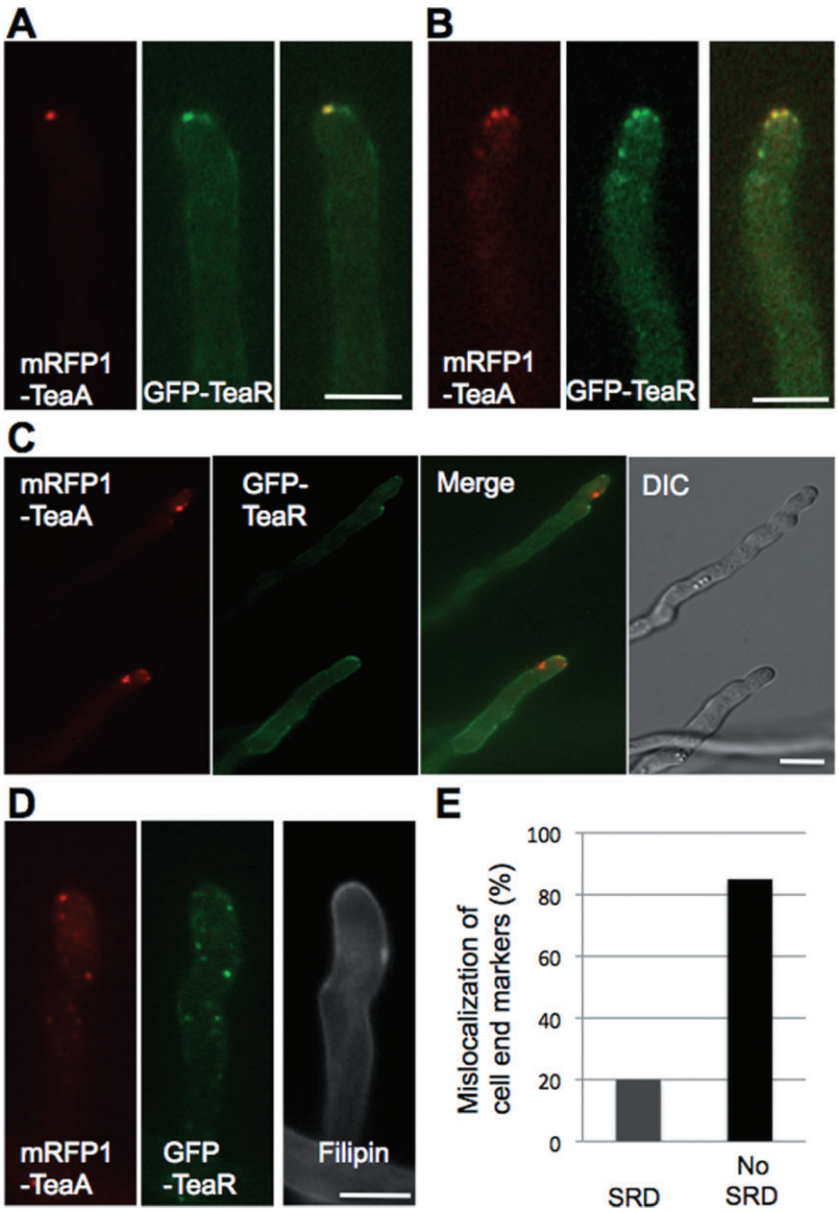

Fig. 5. Localization of cell end markers in a *floA*-deletion strain. (A–D) The strains expressing mRFP1–TeaA and GFP–TeaR in wild type (A and B) and in the *floA*-deletion strain (C and D) were grown in minimal medium with glucose overnight. mRFP1–TeaA and GFP–TeaR colocalized at the hyphal tip apex (A), sometimes located at some spots aligned along the tip apex (B). (C) In the *floA*-deletion strain, TeaA and TeaR sometimes spread to subapical regions and the cortex of backward protrusions and ripples of hyphae. (D) At the tips of hyphae where clear SRDs were not observed, TeaA and TeaR often showed dispersed signals at the subapical cortex. Hyphae were stained using filipin 1 μg ml^{-1} for 5 min. Scale bars = 5 μm. (E) Frequency of the mislocalization of cell end markers to subapical region was measured at tips in the presence or absence of SRDs (n = 100 respectively).

Localization of StoB

Another *A. nidulans* stomatin orthologue, StoB, is comprised of a signal peptide at the N-terminus of StoB and is predicted to localize to mitochondria (analysed by wolf-psort and predSL algorithms). We confirmed the predicted localization of StoB tagged with GFP in mitochondria (Fig. S2). Human stomatin-like protein, STOML-2, also has a mitochondrial localization sequence at its N-terminus and has been found in many cell types in the inner mitochondrial membrane (Wang and Morrow, 2000). StoB showed a higher similarity to STOML-2 (4e-99) than that of stomatin (1e-17); these data indicate that StoB belongs to the stomatin-like protein group. Since StoB is apparently not directly involved in SRD formation, the role of *stoB* was not analysed further.

floA*,* stoA *double deletion*

To analyse the functional relation of FloA and StoA, a *floA*, *stoA* double-deletion strain was constructed. The *floA*, *stoA* double-deletion strain exhibited even slower growth than the *floA*-deletion strain (Fig. 8A). Moreover, the double deletion strain showed severely abnormal hyphae, such as uneven hyphae, depolarized swelling regions and irregular branching patterns (Fig. 8B and C). These phenotypes indicate that tip growth is severely impaired in the double-deletion strain. That is consistent with the result that SRDs were not detected frequently in this strain

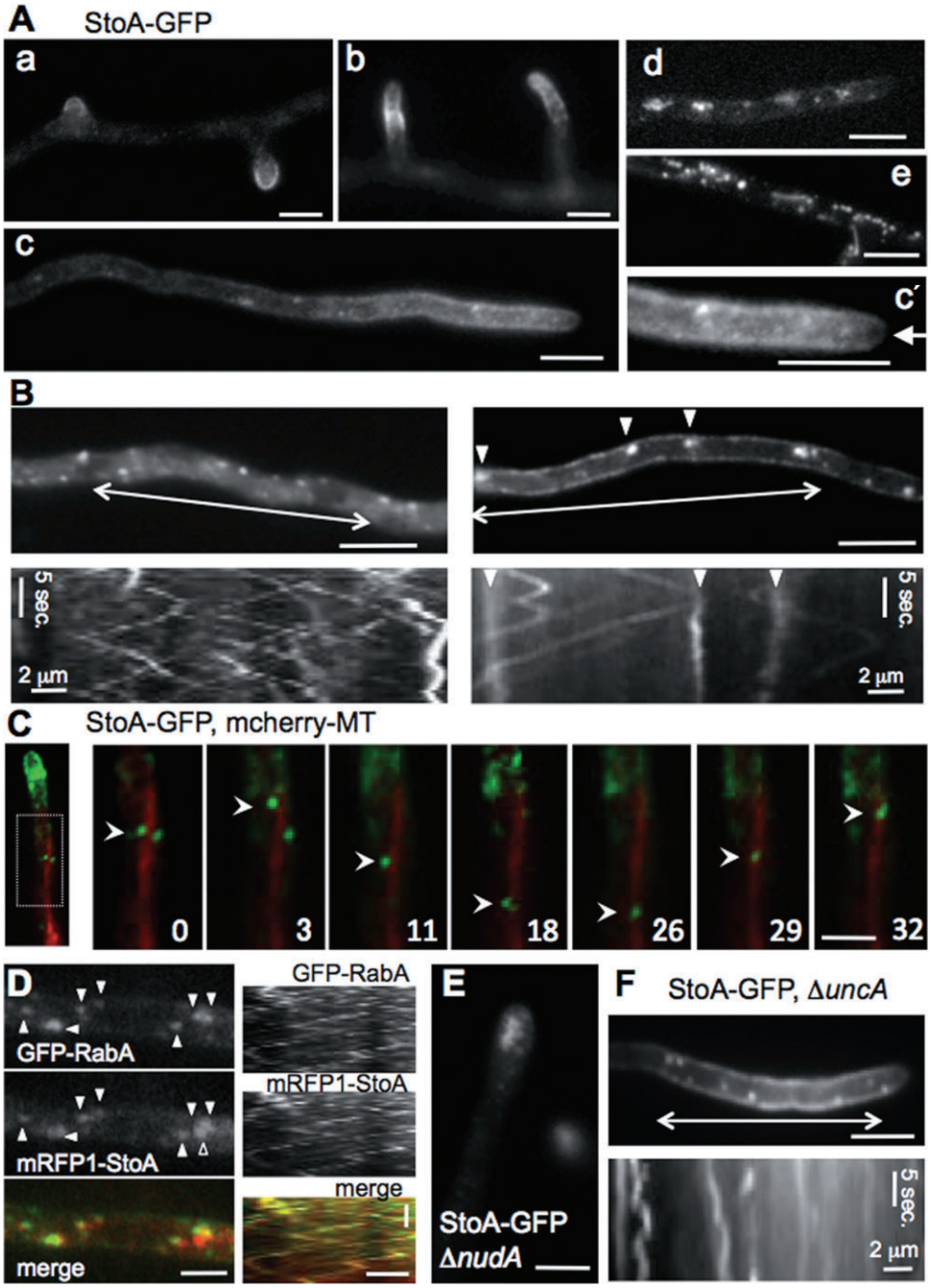

(Fig. 4B). The increased branch formation observed in the *stoA*-deletion strain appeared to be suppressed by deletion of *floA*; on the other hand, swelling of hyphae around septa has been sometimes observed (Fig. 8D arrows and E). The swelling may indicate abnormal branch formation.

Subsequently, we investigated the localization of FloA–GFP in a *stoA*-deletion background and StoA–GFP in a *floA*-deletion background. FloA–GFP localized to the plasma membrane except at hyphal tips in the *stoA*-deletion strain as well as in wild type (Fig. 8F), while StoA–GFP localized at the tip cortex of branches and the subapical cortex of long hyphae in the *floA*-deletion strain (Fig. 8G and H), suggesting that FloA and StoA localize to their proper membrane regions independently.

FloA and StoA association with detergent-resistant membrane regions

The localization of FloA and StoA were further investigated using biochemical methods. The clarified cell lysate (supernatant after centrifugation at 10 000 *g* for 15 min) was centrifuged at 100 000 *g* for 30 min. We used the

Fig. 6. Localization of StoA–GFP.
A. The strain expressing functional StoA tagged with GFP at the C-terminus under the control of the native promoter was grown in minimal medium with glucose overnight. StoA–GFP located at the tip cortex of young branch tips (a), but also dispersed to the subapical cortex, depending on the elongation of branch tips (b). After hyphae reached a certain length, StoA–GFP located to the subapical cortex (c), but not to the apex (c′). In a small number of hyphae, StoA–GFP did not localize at the subapical cortex, but at endosomal structures (d). In old compartments of hyphae, the GFP signal located to vacuole-like structures (e).
B. The smaller spots of StoA–GFP often moved bidirectionally for long distances (left). In contrast, the larger and less abundant spots of StoA–GFP showed only short-range movement (right, arrowheads). Kymographs were made by ImageJ on a segmented line (not shown) inside of hyphae restricted by the arrow line. Vertical bars = 5 s, horizontal bars = 2 μm.
C. The spot of StoA–GFP moved bi-directionally along microtubules (mCherry tagged α-tubulin). Elapsed time is given in seconds. Scale bars = 5 μm.
D. The strain expressing GFP–RabA (marker of endosome) and mRFP1–StoA was grown in minimal medium with glycerol overnight. mRFP1–StoA and GFP–RabA colocalized at the smaller spots (arrowheads) but the larger spots of mRFP1–StoA did not colocalize with GFP–RabA (openarrowhead). Kymographs of GFP–RabA and mRFP1–StoA are shown. Vertical bars = 5 s, horizontal bars = 2 μm.
E. StoA–GFP accumulated at almost all tips in the *nudA*-deletion strain. Scale bars = 5 μm.
F. In the *uncA*-deletion strain, StoA–GFP localized at the subapical cortex and cytoplasmic dots. The dots just oscillated but did not move bidirectionally in long distances. Scale bars = 5 μm. Kymographs were made on a segmented line (not shown) inside of hyphae restricted by the arrow line. Vertical bars = 5 s, horizontal bars = 2 μm.

supernatant as cytoplasmic fraction and the pellet as membrane fraction for protein analysis by Western blotting. As expected, TubA (α-tubulin) was detected in the cytoplasmic fraction, whereas ChsB (chitin synthase, a transmembrane protein) was detected in the membrane fraction (Fig. 9A). Under these conditions, both FloA and StoA were found in the membrane fraction, suggesting that FloA and StoA mainly locate at membranes.

Membrane fragments that are insoluble in non-ionic detergents like Triton X-100 can be isolated from a wide variety of mammalian cell types (Brown and Rose, 1992) and yeast cells (Kubler *et al*., 1996). They were thought to represent the biochemical equivalent of lipid rafts (Wachtler and Balasubramanian, 2006); however, it became clear that detergent-resistant membranes do not define functional membrane rafts (Tanner *et al*., 2011). In order to investigate whether FloA and StoA locate at the detergent-resistant membranes, the membranes were isolated and analysed for the presence of the two proteins. The clarified cell lysate was treated with 2% Triton X-100 for 1 h on ice, and then loaded on a 10–40% sucrose gradient, centrifuged at 100 000 *g* for 3 h and fractionated into seven different samples. Detergent-resistant membranes are known to be enriched in the low-density fraction. Both FloA and StoA were detected exactly in these fractions (Fig. 9B). Unfortunately, we had no positive control for raft-localizing proteins or detergent-resistant membranes; StoA and FloA are – to our knowledge – the first examples of such localizations in filamentous fungi. The prenylated protein TeaR was found at higher density fractions, which is consistent with the accepted idea that prenylated proteins are excluded from rafts (Melkonian *et al*., 1999).

Discussion

Selecting the microdomain-scaffolding protein flotillin/reggie orthologue, FloA, and the related stomatin orthologue, StoA, we analysed their functions by gene deletion and protein localization. This is the first report of a functional characterization of flotillin/reggie and stomatin orthologues in fungi. We tested the possibility that the microdomain-scaffolding protein FloA functions in SRD formation and positioning of cell end marker proteins. Indeed, we found that SRD distribution was altered in hyphal tips of *floA*-deletion strains and the positioning of cell end markers was clearly changed. However, FloA localized at the plasma membrane except at hyphal tips, unexpectedly opposite from SRDs, which are concentrated at hyphal tips. The localization pattern of FloA therefore suggests an indirect function in SRD formation or a direct negative effect on the formation of SRDs, raising the question about the primary function of FloA in *A. nidulans* and probably other filamentous fungi. If we assume that FloA functions as a scaffolding protein, which compartmentalizes the cytoplasmic membrane, one has to assume that these membrane domains consist of different lipids with some specific functions. The FloA–GFP dots aligned along the plasma membrane possibly indicate such membrane domains, which are shown to be stable and immobile. One possibility for such membrane domains is that they are involved in specific endocytosis. This hypothesis is based on findings in mammalian cells, where flotillin is known to be involved in a clathrin- and caveolin-independent endocytic pathway (Glebov *et al*., 2006; Ait-Slimane *et al*., 2009). It is now clear that cells have several endocytic mechanisms. In addition to the classical clathrin-dependent mechanism, several pathways were discovered that do not use a clathrin coat (Mayor and Pagano, 2007; Sandvig *et al*., 2011). Among the clathrin-independent pathways, flotillins were found to be involved in both dynamin-dependent (Ait-Slimane *et al*., 2009) and dynamin-independent uptake (Glebov *et al*., 2006). However, it is not clear yet, if flotillin participates directly in endocytosis, because flotillin may affect the efficiency of uptake by aggregating lipid-associated

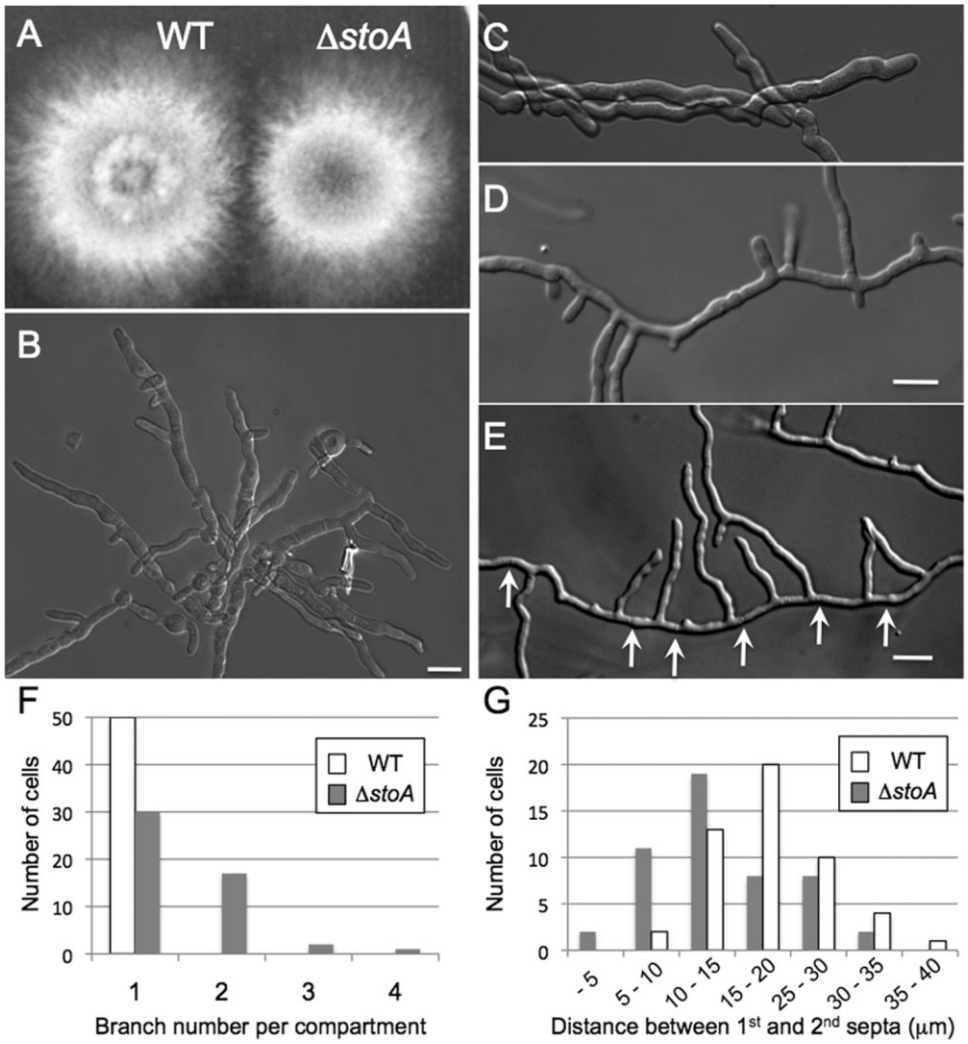

Fig. 7. Deletion of *stoA*.
A. Colonies of wild type (left) and a *stoA*-deletion (right) strain. Strains were grown in minimal medium with glucose agar plates for 3 days at 37°C.
B–E. The *stoA*-deletion strain was grown in minimal medium with glucose overnight at 28°C. Hyphae were thicker, especially in young hyphae (B), and hyphae were irregularly formed (C). Branch formation was higher in the *stoA*-deletion strain (D and E). Scale bars = 10 μm. Arrows indicate septa.
F. Quantification of branch formation. One branch always appeared from one compartment in wild type (open symbols). In contrast, two branches and even three or four were sometimes formed per compartment of the *stoA*-deletion strain (closed symbols) ($n = 50$ respectively).
G. Quantification of the compartment size. The distance between the first and the second septum in germinated hyphae was measured in wild type (open symbols) and the *stoA*-deletion strain (closed symbols) ($n = 50$ respectively).

receptors and certain lipid species at invaginated membrane areas (Langhorst *et al*., 2008; Sandvig *et al*., 2011).

In filamentous fungi, although the clathrin-independent endocytic pathway is not yet clear at all, the essentials of endocytosis for hyphal growth have been revealed (Araujo-Bazan *et al*., 2008; Upadhyay and Shaw, 2008; Peñalva, 2010). At tips of hyphae, exocytosis and endocytosis cooperate spatially; in other words, exocytosis occurs at the apex of hyphae and endocytosis occurs mainly at the subapical region (Araujo-Bazan *et al*., 2008; Taheri-Talesh *et al*., 2008; Berepiki *et al*., 2011). Moreover, roles of endocytic recycling at hyphal tips for polarity maintenance have been suggested (Hervas-Aguilar and Peñalva, 2010; Shaw *et al*., 2011). The localization of FloA at the plasma membrane except at hyphal tips is consistent with the putative specific function of FloA in endocytosis. Interestingly, the localization of FloA is similar to eisosomes in other fungi, which are suggested to form static sites of endocytosis at the plasma membrane (Walther *et al*., 2006; Grossmann *et al*., 2008; Vangelatos *et al*., 2010; Reijnst *et al*., 2011; Seger *et al*., 2011). The question whether FloA is involved in endocy-

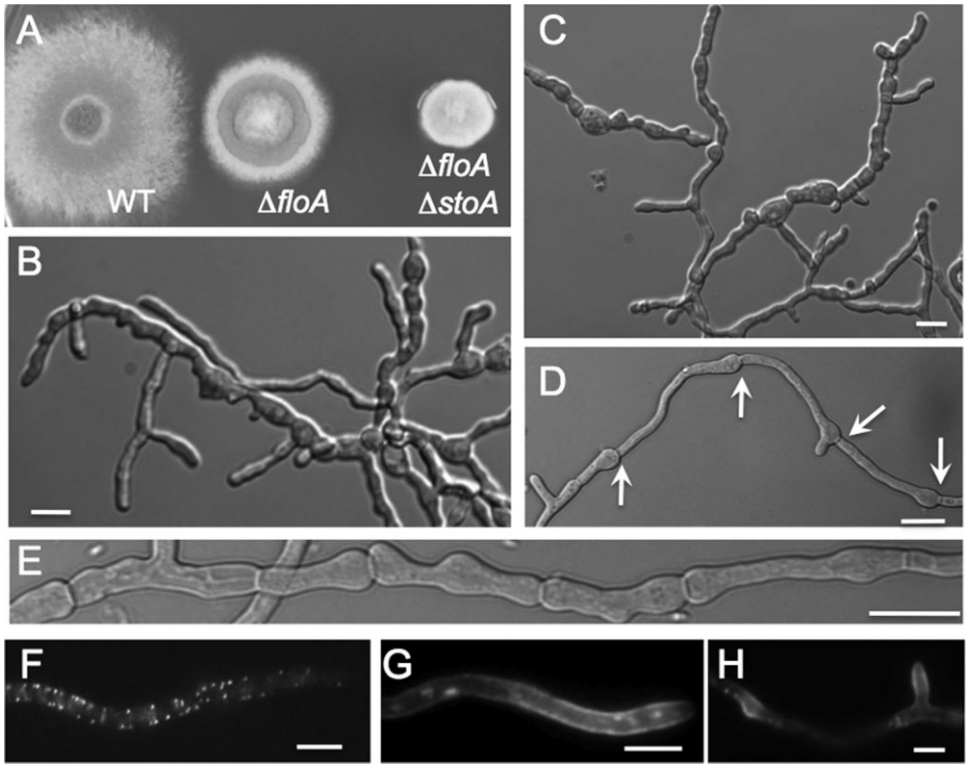

Fig. 8. Double deletion of *floA* and *stoA*.
A. Colonies of wild type (left), the *floA*-deletion (middle), and *floA*, *stoA* double-deletion strain (right). Strains were grown in minimal medium with glucose agar plates for 3 days at 37°C.
B–E. The *floA*, *stoA* double-deletion strain was grown in minimal medium with glucose overnight at 28°C. The double-deletion strain showed severely abnormal morphology of hyphae, such as uneven hyphae, depolarized swelling regions and an irregular branching pattern (B and C). Swelling of hyphae was sometimes observed around septa (D and E). Arrows indicate septa. Scale bars = 10 μm.
F. FloA–GFP localized to stable dots along the plasma membrane except hyphal tip in the *stoA*-deletion strain.
G and H. StoA–GFP localized at the subapical cortex of long hyphae (G) and the tip cortex of branches (H) in the *floA*-deletion strain. Scale bars = 5 μm.

tosis – directly or indirectly – is not solved yet. Preliminary evidence shows that FloA is not involved in the endocytosis of several transporters in *A. nidulans* (E. Fotinou and G. Diallinas, unpublished). If FloA functions in endocytosis, its role will be specific for the internalization of specific cargoes, and should not act as a general endocytic factor affecting polar growth. This idea is compatible with a specific endocytic role responsible for SRD formation or maintenance.

If FloA is not directly involved in the SRD formation, one of course has to ask if there are other FloA-related or completely different proteins which are scaffolding SRDs. Some different pathways, such as the actin cytoskeleton, septin filaments and sterol transport, could be involved in this process. The fact that SRDs are characteristic for fungi could indicate that specific scaffolding proteins exist in these organisms. However, another possibility is that apical SRDs are formed by compartmentalization of subapical membranes. The existence of SRDs at hyphal tips and the localization of FloA at the subapical plasma membrane strongly suggest that the plasma membranes are distinct at hyphal tips and the remaining hyphae. One difference, which could account for the different lipid compositions, could be the curvature of the apical membrane. Besides the physical character of membranes, microdomain-scaffolding proteins such as FloA could be involved in membrane compartmentalization. By structuring the subapical membrane, FloA may be indirectly responsible for the maintenance of SRDs at the tip.

In some cases, such as axon growth, cadherin recruitment at contact sites between cells and migrating neutrophils, flotillins are likely to participate in polar growth by forming membrane domains at polarity sites (Rossy *et al.*, 2009; Stuermer, 2010). In *A. nidulans*, however, FloA does not localize at the polarity cites, i.e. growing hyphal tips, branching sites and forming septa. Interestingly, in plant root hair tips of *Medicago truncatula*, Flotillin orthologue FLOT4 displayed a punctate distribution at the plasma membrane, which in response to symbiotic bacteria redistributed to form a cap at the cell tip (Haney and Long, 2010). A receptor kinase for the bacterial infection is involved in the localization change of FLOT4 (Haney

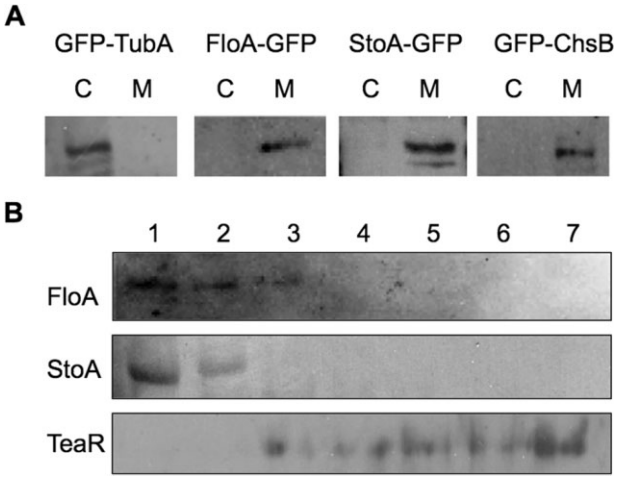

Fig. 9. FloA and StoA association with detergent-resistant membranes.
A. The clarified cell lysate was centrifuged at 100 000 *g* for 30 min to separate the cytoplasm from the cell membrane fraction. The fractions were analysed by immunoblotting with the anti-GFP antibody. TubA (α-tubulin) is a marker for the cytoplasmic fraction, whereas ChsB (chitin synthase, transmembrane protein) is a marker for the membrane fraction. Under these conditions, both FloA and StoA were identified in the membrane fraction.
B. The clarified cell lysate was treated with 2% Triton X-100 for 1 h on ice, and then carefully added to the top of a 10–40% sucrose gradient, centrifuged at 100 000 *g* for 3 h, and fractionated 1 to 7. The fractions were analysed by immunoblotting using the anti-GFP antibody. Both FloA and StoA were detected in low-density fractions (1, 2); in contrast, the prenylated protein TeaR was found in higher-density fractions.

et al., 2011). Our localization studies with the truncated FloA version might be the first hints to localization changes of FloA and a membrane restructuring during certain conditions.

In addition to an effect of *floA* deletion on SRD maintenance, we found an effect on cell end marker positioning. This effect could also be due to defects in endocytosis. Another possibility is that microdomains in SRDs affect directly localization of proteins at the membrane. Besides cell end markers, SRDs are known to be necessary for the localization of other components of the growth machinery, such as formin (Pearson *et al*., 2004; Canovas and Perez-Martin, 2009). To investigate deeply the relation of lipid membrane domains and protein localization, the distribution of microdomains within SRDs has to be resolved. Although the uniform filipin-staining signal along the apex of hyphae suggests homogeneity, there should be not only raft membranes but also non-raft membranes at hyphal tips. This could account for TeaR localization, because there is evidence that prenylated proteins are excluded from rafts and be inserted preferentially in non-raft membranes (Melkonian *et al*., 1999) (Fig. 5B). The size of SRDs is around a few μm, whereas the size of lipid rafts ranges in general between 10–200 nm (Pike, 2009). SRDs are predicted to be composed of a mozaic pattern of raft membranes and non-raft membranes. At present, one substantial limitation is the diffraction limit of the resolution when using conventional microscopy, whose resolution limit is 250 nm. In recent years, super-resolution microscope techniques have been improving and breaking the diffraction limit of conventional light microscopy (Galbraith and Galbraith, 2011). In this method, a lateral image resolution as high as 20 nm will be a powerful tool to investigate membrane microdomains (Rust *et al*., 2006).

Two other SPFH proteins belonging to the stomatin family of proteins were also analysed in this paper. While stomatin is conserved in bacteria and many eukaryotes, it is not found in *S. cerevisiae* or *S. pombe* (Green and Young, 2008). StoA located at the tip cortex of branches or the subapical cortex of hyphae. By contrast, StoB located at mitochondria, which may be reminiscent of stomatin in prokaryotes. The localization change of StoA at the tip cortex of young branches and subapical cortex in long hyphae could be regulated by endocytosis, because StoA is transported on endosomes, which are thought to serve as a platform for endocytic vesicles. Moreover, the localization change of StoA might indicate the difference of membrane domains at branch tips and at growing hyphal tips, such as raft clustering or the ratio of each lipid. In mammalian cells, since different SPFH proteins function on different organelle membranes, each SPFH protein is thought to possess common functions on each membrane (Browman *et al*., 2007). Likewise, in *A. nidulans*, FloA and StoA might share common functions on different membranes at the subapical cortex, branch tip cortex and endosomes.

Although the functions of FloA and StoA at the molecular level are not clear yet, the severe morphological phenotype in the *floA*, *stoA* double-deletion strain indicate the importance of their putative functions for microdomain formation in tip growth. The facts that StoA localized at branch tips and that the deletion of *stoA* increased branch formation suggest the functions in branch formation. Without StoA, microdomains probably will not cluster properly at branch emerging sites, which can be expected to lead to reduced clustering of certain proteins. Rather, those proteins required for branching would be localized along the hyphae and induce abnormal branch formation. On the other hand, increasing branch formation by deletion of *stoA* was suppressed by deletion of *floA*, suggesting the ratio of FloA and StoA matters for branch formation.

In summary, we analysed the roles of the microdomain-scaffolding protein flotillin/reggie orthologues FloA and the related protein Stomatin orthologue StoA. The exact mechanism how SRDs are formed is not yet revealed. The next challenge will be to identify the factors directly involved in SRD formation, to visualize membrane domains in SRDs and to study the link between SRD

formation and cell cytoskeleton functions and signal transduction as well as with exo- and endocytosis to get a comprehensive understanding of polarized growth. Finally, in the present work, we did not address flotillin evolution, which is very interesting by itself and is going to be addressed elsewhere.

Experimental procedures

Strains, plasmids and culture conditions

Supplemented minimal medium for *A. nidulans* was prepared as described, and standard strain construction procedures were used (Hill and Kafer, 2001; http://www.fgsc.net/fgn48/Hill.htm). Two per cent of glucose was used as carbon source, and 70 mM sodium nitrate and 0.9 μM ammonium molybdate were used as nitrogen source. *A. nidulans* strains used in this study are listed in Table S1. Standard laboratory *Escherichia coli* strains (XL-1 blue, Top 10 F') were used. Plasmids are listed in Table S2.

Molecular techniques

Standard DNA transformation procedures were used for *A. nidulans* and *E. coli*. For PCR experiments, standard protocols were applied using a personal Cycler (Biometra) for the reaction cycles. DNA sequencing was performed commercially (MWG Biotech, Ebersberg, Germany). DNA analyses and Southern hybridizations were performed as described by Sambrook and Russel (1999).

Tagging with GFP or HA and gene deletion

StoA and StoB were tagged with GFP at the C-terminal end. The 1 kb C-terminal region of the gene with primers P4 and P6, and the 1 kb terminator region of the gene with primers P5 and P8 were amplified respectively (primer list is shown in Table S3). A fragment of the GFP–pyrG cassette was amplified from pFNO3 using primers Sfi-GFP-for and Sfi-pyrG-rev; the primer P6, P5, Sfi-GFP-for and Sfi-pyrG-rev include SfiI sites. The three fragments were digested by SfiI and ligated. The three ligated fragments were amplified with primers P4 and P7. PCR products for the FloAΔC–GFP construction were amplified by the same strategy. The PCR products were transformed into uridine/uracil-auxotrophic *A. nidulans* Δ*nkuA* strain TN02A3, in order to increase the frequency of homologues integration.

For tagging FloA with GFP at the C-teminus, the full length of *floA* was amplified with primers KpnI-floA-for and floA-rev-GFP-link. GFP was amplified with primers GFP-for-floA-link and PacI-GFP-rev. Using the PCR products of *floA* and GFP as templates, FloA–GFP flagment was amplified with primers KpnI-floA-for and PacI-GFP-rev, was digested by KpnI and PacI, and was subcloned into KpnI-PacI digested pCMB17apx, yielding pNT61 ($alcA_{(p)}$–FloA–GFP). The *alcA* promoter of pNT61 was replaced by 2 kb *floA* promoter. The promoter region was amplified with primers flo-pro-EI-f and flo-pro-kpn-re, was digested by EcoRI and KpnI, and was subcloned into EcoRI-KpnI digested pNT61, yielding pNT62 ($floA_{(p)}$–FloA–GFP). For tagging FloA with three repeats HA tag at the N-terminus, the full length of *floA* was amplified with primers AscI-floA and PacI-floA was digested by AscI and PacI, and was subcloned into AscI-PacI digested pSM14, yielding pNT63 ($alcA_{(p)}$–3xHA–FloA). The promoter region of *floA* was amplified with primers flo-pro-EI-f and flo-pro-kpn-re, was digested by EcoRI and KpnI, and was subcloned into EcoRI-KpnI digested pNT63, yielding pNT64 ($floA_{(p)}$–3xHA–FloA).

For tagging FloA and StoA with GFP at the N-terminus, the 1 kb N-terminal region of the gene was amplified with primers Efi-for and Efi-re, and then cloned into a cloning vector. The AscI-PacI fragment was subcloned into pCMB17apx, yielding pNT58 (GFP–FloA) and pNT59 (GFP–StoA). The plasmids were transformed into the TN02A3 strain.

To delete *floA*, *stoA* and *stoB*, the 1 kb promoter region of gene was amplified with primers P1 and P3. A fragment of the *pyrG* marker cassette was amplified with primers Sfi-pyrG-for and Sfi-pyrG-rev; the primer P1, Sfi-pyrG-for and Sfi-pyrG-rev included SfiI sites. PCR products of the promoter region, *pryG*, and the terminator region amplified by P5 and P8, were first digested using SfiI and then ligated. The three ligated fragments were amplified with primers P2 and P7. The PCR products were transformed into the TN02A3 strain.

The primary transformants were screened microscopically and by PCR for correct integration of the GFP tagging or deletion cassette. Integration events were confirmed by Southern blotting.

Light/fluorescence microscopy

Live-cell imaging of germlings and young hyphae: cells were grown on coverslips in 0.5 ml minimal medium + 2% glucose. When we observe strains expressing gene of interest under inducible *alcA* promoter, minimal medium + 2% glycerol (derepression of the *alcA* promoter) were used. Cells were incubated at 30°C for overnight or 1 day. The coverslips were mounted on slide glass. Tempcontrol mini (Pepcon) was used as needed to keep temperature of the slide glass during microscopy. Images were captured using an Axiophot microscope using a Planapochromatic 63 times oil immersion objective lens, the Zeiss AxioCam MRM camera (Zeiss, Jena, Germany), and the HBO103 mercury arc lamp (Osram) or HXP 120 (Zeiss, Jena, Germany) possessing faster speed wavelength switching. Images were collected and analysed using the AxioVision system (Zeiss). Kymographs were made using ImageJ software (http://rsb.info.nih.gov/ij/).

Filipin, benomyl and cytochalasin A treatment

Filipin (Sigma, Deisenhofen) was used at a final concentration of 1 μg ml^{-1} in medium from a stock solution of 10 mg ml^{-1} in dimethylsulphoxide (DMSO). Benomyl, methyl 1-(butylcarbamoyl)-2-benzimidazole carbamate (Aldrich) was used at a final concentration of 2 μg ml^{-1} in medium from a stock solution of 1 mg ml^{-1} in ethanol. Cytochalasin A (Sigma) was used at a final concentration of 2 μg ml^{-1} in medium from a stock solution of 100 mg ml^{-1} in DMSO.

Indirect immunofluorescent staining

Spores of SNT123 were grown on coverslips in 0.5 ml minimal medium + 2% glucose at 30°C for overnight. Cells grown on coverslips were fixed with 3.7% formaldehyde in PBS buffer at room temperature for 30 min. The coverslips were washed by 0.1% tween 20 in PBS buffer (PBS-T) and treated by 200 μl cell wall-digestion solution [30 mg ml^{-1} glucanex (novozymes) in PBS] at 30°C for 30 min. The coverslips were washed by PBS-T three times and incubated with a mouse anti-HA primary antibody (Covance) at 1:200 dilution in 0.1% BSA in PBS solution at room temperature for 1 h. The coverslips were washed by PBS-T three times and incubated with a FITC-conjugated anti-mouse IgG secondary antibody (Sigma) at 1:500 dilution in 0.1% BSA in PBS solution at room temperature for 1 h in the dark. The coverslips were washed by PBS-T three times, mounted on glass slides and observed by the fluorescent microscopy.

Subcellular fractionation and detergent-resistant membrane isolation

Aspergillus nidulans strains were cultured in minimal medium containing 2% threonine and 0.2% glucose for 24 h in order to overexpress GFP–TubA, FloA–GFP and GFP–ChsB expressed under *alcA* promoter. The mycelium was ground in liquid nitrogen, resuspended in protein extraction buffer [50 mM Tris-HCl (pH 7.4), 150 mM NaCl, 5 mM EDTA], supplemented with a cocktail of protease inhibitor (Sigma) and centrifuged at 10 000 *g* for 15 min. The supernatant (clarified cell lysate) was centrifuged at 100 000 *g* for 30 min. We used the supernatant as the cytoplasmic fraction and the pellet as the membrane fraction for Western blotting analysis, using anti-GFP antibody.

In order to isolate detergent-resistant membranes, the clarified cell lysate was treated with 2% Triton X-100 for 1 h on ice, and then loaded on the 10–40% sucrose gradient (two-step gradient 10 or 40% sucrose in the protein extraction buffer), and centrifuged at 100 000 *g* for 3 h. Six fractions of equal volume were collected from the top of the gradient (1–6), and the pellet fraction was used as 7. The fractions were analysed using Western blotting analysis with anti-GFP antibody.

Acknowledgements

We kindly thank Xin Xiang (Uniformed Services University, USA) for the *nudA*-deletion strain, Stephen Osmani (Ohio State University, USA) for the plasmid containing the GFP–pyrG cassette, Miguel Peñalva (CESIC, Madrid, Spain) for the GFP–RabA plasmid. We also thank Sotiris Amillis for communicating results based on a strain expressing a *gpdA* promoter driven *floA* gene and an independent *floAΔ* null mutant. This work was supported by the DFG and the Baden-Württemberg Stiftung. N.T. is a Humboldt fellow. We thank C. Stürmer (University of Konstanz, Germany) for stimulating discussions at the beginning of the project.

References

Abenza, J.F., Pantazopoulou, A., Rodriguez, J.M., Galindo, A., and Peñalva, M.A. (2009) Long-distance movement of *Aspergillus nidulans* early endosomes on microtubule tracks. *Traffic* **10:** 57–75.

Abenza, J.F., Galindo, A., Pantazopoulou, A., Gil, C., de los Rios, V., and Peñalva, M.A. (2010) *Aspergillus* RabB Rab5 integrates acquisition of degradative identity with the long distance movement of early endosomes. *Mol Biol Cell* **21:** 2756–2769.

Ait-Slimane, T., Galmes, R., Trugnan, G., and Maurice, M. (2009) Basolateral internalization of GPI-anchored proteins occurs via a clathrin-independent flotillin-dependent pathway in polarized hepatic cells. *Mol Biol Cell* **20:** 3792–3800.

Alvarez, F.J., Douglas, L.M., and Konopka, J.B. (2007) Sterol-rich plasma membrane domains in fungi. *Eukaryot Cell* **6:** 755–763.

Araujo-Bazan, L., Peñalva, M.A., and Espeso, E.A. (2008) Preferential localization of the endocytic internalization machinery to hyphal tips underlies polarization of the actin cytoskeleton in *Aspergillus nidulans*. *Mol Microbiol* **67:** 891–905.

Babuke, T., and Tikkanen, R. (2007) Dissecting the molecular function of reggie/flotillin proteins. *Eur J Cell Biol* **86:** 525–532.

Bagnat, M., and Simons, K. (2002) Cell surface polarization during yeast mating. *Proc Natl Acad Sci USA* **99:** 14183–14188.

Baumann, N.A., Sullivan, D., Ohvo-Rekila, H., Simonot, C., Pottekat, A., Klaassen, Z., *et al*. (2005) Transport of newly synthesized sterol to the sterol-enriched plasma membrane occurs via nonvesicular equilibration. *Biochemistry* **44:** 5816–5826.

Berepiki, A., Lichius, A., and Read, N.D. (2011) Actin organization and dynamics in filamentous fungi. *Nat Rev Microbiol* **9:** 876–887.

Bickel, P.E., Scherer, P.E., Schnitzer, J.E., Oh, P., Lisanti, M., and Lodish, H.F. (1997) Flotillin and epidermal surface antigen define a new family of caveolae-associated integral membrane proteins. *J Biol Chem* **272:** 13793–13802.

Borner, G.H., Sherrier, D.J., Weimar, T., Michaelson, L.V., Hawkins, N.D., Macaskill, A., *et al*. (2005) Analysis of detergent-resistant membranes in Arabidopsis. Evidence for plasma membrane lipid rafts. *Plant Physiol* **137:** 104–116.

Browman, D.T., Hoegg, M.B., and Robbins, S.M. (2007) The SPFH domain-containing proteins: more than lipid raft markers. *Trends Cell Biol* **17:** 394–402.

Brown, D.A., and Rose, J.K. (1992) Sorting of GPI-anchored proteins to glycolipid-enriched membrane subdomains during transport to the apical cell surface. *Cell* **68:** 533–544.

Canovas, D., and Perez-Martin, J. (2009) Sphingolipid biosynthesis is required for polar growth in the dimorphic phytopathogen *Ustilago maydis*. *Fungal Genet Biol* **46:** 190–200.

Fischer, R., Zekert, N., and Takeshita, N. (2008) Polarized growth in fungi – interplay between the cytoskeleton, positional markers and membrane domains. *Mol Microbiol* **68:** 813–826.

Galbraith, C.G., and Galbraith, J.A. (2011) Super-resolution microscopy at a glance. *J Cell Sci* **124:** 1607–1611.

Glebov, O.O., Bright, N.A., and Nichols, B.J. (2006) Flotillin-1

defines a clathrin-independent endocytic pathway in mammalian cells. *Nat Cell Biol* **8:** 46–54.
Green, J.B., and Young, J. (2008) Slipins: ancient origin, duplication and diversification of the stomatin protein family. *BMC Evol Biol* **8:** 44.
Grossmann, G., Malinsky, J., Stahlschmidt, W., Loibl, M., Weig-Meckl, I., Frommer, W.B., *et al*. (2008) Plasma membrane microdomains regulate turnover of transport proteins in yeast. *J Cell Biol* **183:** 1075–1088.
Haney, C.H., and Long, S.R. (2010) Plant flotillins are required for infection by nitrogen-fixing bacteria. *Proc Natl Acad Sci USA* **107:** 478–483.
Haney, C.H., Riely, B.K., Tricoli, D.M., Cook, D.R., Ehrhardt, D.W., and Long, S.R. (2011) Symbiotic rhizobia bacteria trigger a change in localization and dynamics of the *Medicago truncatula* receptor kinase LYK3. *Plant Cell* **23:** 2774–2787.
Harold, F.M. (1999) In pursuit of the whole hypha. *Fungal Genet Biol* **27:** 128–133.
Hervas-Aguilar, A., and Peñalva, M.A. (2010) Endocytic machinery protein SlaB is dispensable for polarity establishment but necessary for polarity maintenance in hyphal tip cells of *Aspergillus nidulans*. *Eukaryot Cell* **9:** 1504–1518.
Higashitsuji, Y., Herrero, S., Takeshita, N., and Fischer, R. (2009) The cell end marker protein TeaC is involved in growth directionality and septation in *Aspergillus nidulans*. *Eukaryot Cell* **8:** 957–967.
Hill, T.W., and Kafer, E. (2001) Improved protocols for Aspergillus minimal medium: trace element and minimal medium salt stock solutions. *Fungal Genet Newsl* **48:** 20–21.
Hinderhofer, M., Walker, C.A., Friemel, A., Stuermer, C.A., Moller, H.M., and Reuter, A. (2009) Evolution of prokaryotic SPFH proteins. *BMC Evol Biol* **9:** 10.
Kubler, E., Dohlman, H.G., and Lisanti, M. (1996) Identification of Triton X-100 insoluble membrane domains in the yeast *Saccharomyces cerevisiae*. Lipid requirements for targeting of heterotrimeric G-protein subunits. *J Biol Chem* **271:** 32975–32980.
Langhorst, M.F., Reuter, A., Jaeger, F.A., Wippich, F.M., Luxenhofer, G., Plattner, H., and Stuermer, C.A. (2008) Trafficking of the microdomain scaffolding protein reggie-1/flotillin-2. *Eur J Cell Biol* **87:** 211–226.
Li, S., Du, L., Yuen, G., and Harris, S.D. (2006) Distinct ceramide synthases regulate polarized growth in the filamentous fungus *Aspergillus nidulans*. *Mol Biol Cell* **17:** 1218–1227.
Lingwood, D., and Simons, K. (2010) Lipid rafts as a membrane-organizing principle. *Science* **327:** 46–50.
Mairhofer, M., Steiner, M., Salzer, U., and Prohaska, R. (2009) Stomatin-like protein-1 interacts with stomatin and is targeted to late endosomes. *J Biol Chem* **284:** 29218–29229.
Mania, D., Hilpert, K., Ruden, S., Fischer, R., and Takeshita, N. (2010) Screening for antifungal peptides and their modes of action in *Aspergillus nidulans*. *Appl Environ Microbiol* **76:** 7102–7108.
Martin, S.W., and Konopka, J.B. (2004) Lipid raft polarization contributes to hyphal growth in *Candida albicans*. *Eukaryot Cell* **3:** 675–684.
Mayor, S., and Pagano, R.E. (2007) Pathways of clathrin-independent endocytosis. *Nat Rev Mol Cell Biol* **8:** 603–612.
Melkonian, K.A., Ostermeyer, A.G., Chen, J.Z., Roth, M.G., and Brown, D.A. (1999) Role of lipid modifications in targeting proteins to detergent-resistant membrane rafts. Many raft proteins are acylated, while few are prenylated. *J Biol Chem* **274:** 3910–3917.
Mishra, S., Murphy, L.C., and Murphy, L.J. (2006) The Prohibitins: emerging roles in diverse functions. *J Cell Mol Med* **10:** 353–363.
Morrow, I.C., and Parton, R.G. (2005) Flotillins and the PHB domain protein family: rafts, worms and anaesthetics. *Traffic* **6:** 725–740.
Morrow, I.C., Rea, S., Martin, S., Prior, I.A., Prohaska, R., Hancock, J.F., *et al*. (2002) Flotillin-1/reggie-2 traffics to surface raft domains via a novel golgi-independent pathway. Identification of a novel membrane targeting domain and a role for palmitoylation. *J Biol Chem* **277:** 48834–48841.
Munderloh, C., Solis, G., Bodrikov, V., Jaeger, F.A., Wiechers, M., Malaga-Trillo, E., and Stuermer, C.A. (2009) Reggies/flotillins regulate retinal axon regeneration in the zebrafish optic nerve and differentiation of hippocampal and N2a neurons. *J Neurosci* **29:** 6607–6615.
Nichols, C.B., Fraser, J.A., and Heitman, J. (2004) PAK kinases Ste20 and Pak1 govern cell polarity at different stages of mating in *Cryptococcus neoformans*. *Mol Biol Cell* **15:** 4476–4489.
Pearson, C.L., Xu, K., Sharpless, K.E., and Harris, S.D. (2004) MesA, a novel fungal protein required for the stabilization of polarity axes in *Aspergillus nidulans*. *Mol Biol Cell* **15:** 3658–3672.
Peñalva, M.A. (2010) Endocytosis in filamentous fungi: Cinderella gets her reward. *Curr Opin Microbiol* **13:** 684–692.
Pike, L.J. (2009) The challenge of lipid rafts. *J Lipid Res* **50** (Suppl.): S323–S328.
Rajendra, L., and Simons, K. (2005) Lipid rafts and membrane dynamics. *J Cell Sci* **118:** 1099–1102.
Reijnst, P., Walther, A., and Wendland, J. (2011) Dual-colour fluorescence microscopy using yEmCherry-/GFP-tagging of eisosome components Pil1 and Lsp1 in *Candida albicans*. *Yeast* **28:** 331–338.
Rossy, J., Schlicht, D., Engelhardt, B., and Niggli, V. (2009) Flotillins interact with PSGL-1 in neutrophils and, upon stimulation, rapidly organize into membrane domains subsequently accumulating in the uropod. *PLoS ONE* **4:** e5403.
Rothberg, K.G., Ying, Y.-S., Kamen, B.A., and Anderson, R.G.W. (1990) Cholesterol controls the clustering of the glycophospholipid-anchored membrane receptor for 5-methoyltetrahydrofolate. *J Cell Biol* **111:** 2931–2938.
Rust, M.J., Bates, M., and Zhuang, X. (2006) Sub-diffraction-limit imaging by stochastic optical reconstruction microscopy (STORM). *Nat Methods* **3:** 793–795.
Sambrook, J., and Russel, D.W. (1999) *Molecular Cloning: A Laboratory Manual*. Cold Spring Harbor, NY: Cold Spring Harbor Laboratory Press.
Sandvig, K., Pust, S., Skotland, T., and van Deurs, B. (2011) Clathrin-independent endocytosis: mechanisms and function. *Curr Opin Cell Biol* **23:** 413–420.

Santamaria, A., Castellanos, E., Gomez, V., Benedit, P., Renau-Piqueras, J., Morote, J., *et al.* (2005) PTOV1 enables the nuclear translocation and mitogenic activity of flotillin-1, a major protein of lipid rafts. *Mol Cell Biol* **25:** 1900–1911.

Schuck, S., and Simons, K. (2004) Polarized sorting in epithelial cells: raft clustering and the biogenesis of the apical membrane. *J Cell Sci* **117:** 5955–5964.

Schuster, M., Kilaru, S., Fink, G., Collemare, J., Roger, Y., and Steinberg, G. (2011) Kinesin-3 and dynein cooperate in long-range retrograde endosome motility along a nonuniform microtubule array. *Mol Biol Cell* **22:** 3645–3657.

Seger, S., Rischatsch, R., and Philippsen, P. (2011) Formation and stability of eisosomes in the filamentous fungus *Ashbya gossypii*. *J Cell Sci* **124:** 1629–1634.

Shaw, B.D., Chung, D.W., Wang, C.L., Quintanilla, L.A., and Upadhyay, S. (2011) A role for endocytic recycling in hyphal growth. *Fungal Biol* **115:** 541–546.

Simons, K., and Toomre, D. (2000) Lipid rafts and signal transduction. *Nat Rev Mol Cell Biol* **1:** 31–39.

Snyers, L., Umlauf, E., and Prohaska, R. (1998) Oligomeric nature of the integral membrane protein stomatin. *J Biol Chem* **273:** 17221–17226.

Snyers, L., Umlauf, E., and Prohaska, R. (1999) Association of stomatin with lipid-protein complexes in the plasma membrane and the endocytic compartment. *Eur J Cell Biol* **78:** 802–812.

Steinberg, G. (2011) Motors in fungal morphogenesis: cooperation versus competition. *Curr Opin Microbiol* **6:** 660–667.

Stuermer, C.A. (2010) The reggie/flotillin connection to growth. *Trends Cell Biol* **20:** 6–13.

Stuermer, C.A. (2011) Reggie/flotillin and the targeted delivery of cargo. *J Neurochem* **116:** 708–713.

Szewczyk, E., Nayak, T., Oakley, C.E., Edgerton, H., Xiong, Y., Taheri-Talesh, N., *et al.* (2006) Fusion PCR and gene targeting in *Aspergillus nidulans*. *Nat Protoc* **1:** 3111–3120.

Taheri-Talesh, N., Horio, T., Araujo-Bazan, L., Dou, X., Espeso, E.A., Peñalva, M.A., *et al.* (2008) The tip growth apparatus of *Aspergillus nidulans*. *Mol Biol Cell* **19:** 1439–1449.

Takeshita, N., and Fischer, R. (2011) On the role of microtubules, cell end markers, and septal microtubule organizing centres on site selection for polar growth in *Aspergillus nidulans*. *Fungal Biol* **115:** 506–517.

Takeshita, N., Higashitsuji, Y., Konzack, S., and Fischer, R. (2008) Apical sterol-rich membranes are essential for localizing cell end markers that determine growth directionality in the filamentous fungus *Aspergillus nidulans*. *Mol Biol Cell* **19:** 339–351.

Tanner, W., Malinsky, J., and Opekarova, M. (2011) In plant and animal cells, detergent-resistant membranes do not define functional membrane rafts. *Plant Cell* **23:** 1191–1193.

Upadhyay, S., and Shaw, B.D. (2008) The role of actin, fimbrin and endocytosis in growth of hyphae in *Aspergillus nidulans*. *Mol Microbiol* **68:** 690–705.

Urbani, L., and Simoni, R.D. (1990) Cholesterol and vesicular stomatitis virus G protein take separate routes from the endoplasmic reticulum to the plasma membrane. *J Biol Chem* **265:** 1919–1923.

Vangelatos, I., Roumelioti, K., Gournas, C., Suarez, T., Scazzocchio, C., and Sophianopoulou, V. (2010) Eisosome organization in the filamentous ascomycete *Aspergillus nidulans*. *Eukaryot Cell* **9:** 1441–1454.

Wachtler, V., and Balasubramanian, M.K. (2006) Yeast lipid rafts? – an emerging view. *Trends Cell Biol* **16:** 1–4.

Wachtler, V., Rajagopalan, S., and Balasubramanian, M.K. (2003) Sterol-rich plasma membrane domains in the fission yeast *Schizosaccharomyces pombe*. *J Cell Sci* **116:** 867–874.

Walther, T.C., Brickner, J.H., Aguilar, P.S., Bernales, S., Pantoja, C., and Walter, P. (2006) Eisosomes mark static sites of endocytosis. *Nature* **439:** 998–1003.

Wang, Y., and Morrow, J.S. (2000) Identification and characterization of human SLP-2, a novel homologue of stomatin (band 7.2b) present in erythrocytes and other tissues. *J Biol Chem* **275:** 8062–8071.

Xu, X., Bittman, R., Duportail, G., Heissler, D., Vilcheze, C., and London, E. (2001) Effect of the structure of natural sterols and sphingolipids on the formation of ordered sphingolipid/sterol domains (rafts). Comparison of cholesterol to plant, fungal, and disease-associated sterols and comparison of sphingomyelin, cerebrosides, and ceramide. *J Biol Chem* **276:** 33540–33546.

Zekert, N., and Fischer, R. (2009) The *Aspergillus nidulans* kinesin-3 UncA motor moves vesicles along a subpopulation of microtubules. *Mol Biol Cell* **20:** 673–684.

Supporting information

Additional supporting information may be found in the online version of this article.

Please note: Wiley-Blackwell are not responsible for the content or functionality of any supporting materials supplied by the authors. Any queries (other than missing material) should be directed to the corresponding author for the article.